A Case Study of Ionic Components in the Size-resolved Ambient Particles Collected Near the Volcanic Crater of Sakurajima, Japan

Chang-Jin Ma*, Ki-Hyun Kim[1] and Gong-Unn Kang[2]

Department of Environmental Science, Fukuoka Women's University, Japan
[1]Department of Environment & Energy, Sejong University, Korea
[2]Department of Medical Administration, Wonkwang Health Science University, Korea

*Corresponding author. Tel: +81-92-661-2411 (ext.373), E-mail: ma@fwu.ac.jp

ABSTRACT

In this study, the ionic composition of volcanogenically derived particles and their temporal and spatial distributions have been investigated to evaluate the impact of the volcanic eruption on the local ecosystem and residents. To this end, an intensive field study was conducted to measure the size-segregated particulate matters at the east part of Sakurajima in Japan. Fractionated sampling of particles into $>PM_{10}$, $PM_{10-2.5}$, and $PM_{2.5}$ was made by a multi nozzle cascade impactor (MCI). The concentration of various ions present in the size-resolved particles was determined by Ion chromatography. The time dependent 3-dimensional Volcanic Ash Forecast Transport And Dispersion (VAFTAD) model developed by the NOAA Air Resources Laboratory (ARL) indicated that the sampling site of this work was affected by the volcanic aerosol particles plume. The temporal distributions of sulfate and $PM_{2.5}$ during the field campaign were significantly variable with important contributions to particle mass concentration. The chlorine loss, suspected to be caused by acidic components of volcanic gases, occurred predominantly in fine particles smaller than 10 μm.

Key words: Sakurajima, Volcano, Size-resolved particle, Ionic component, Chlorine loss

1. INTRODUCTION

Sakurajima (31°35′N, 130°39′E) (Fig. 1) is a volcanic island located in the bosom of Kagosima bay of Kyusyu, Japan. Sakurajima is one of the most active volcanoes in Japan. It has erupted several times in recent history. The maximum eruption of volcanic aerosol particles emitted from Sakurajima volcano amount to 29×10^6 t in 1985. The most abundant gas typically released into the atmosphere from volcanism is water vapor, followed by carbon dioxide and sulfur dioxide (Iino and Terada, 2003; Luria *et al*., 1996). Volcanic eruption also releases small amounts of other trace components, including hydrogen, hydrogen sulfide, hydrogen chloride, carbon monoxide, hydrogen fluoride, and helium.

The effects of volcanogenic SO_2 on residents and the environment vary widely depending on (a) the quantity of its emission from crater; (b) the range of its injection (e.g., into the troposphere or stratosphere); and (c) the regional or global meteorological conditions that control its disperse (Bates *et al*., 1987). These SO_2 can be carried to the ground in the form of acid rain or snow after being converted into sulfuric acid (H_2SO_4). Acid rain has been implicated in contributing to forest degradation. There is good reason to believe that acid rain has induced long-term changes in the chemistry of some sensitive soils. The impact of acid rain on forest in Sakurajima was realized, as nearly all trees growing at the downwind section in the Mt. Sakurajima dried up.

About half of the acidity in the atmosphere falls back to earth through dry deposition as gases and dry particles. The particles containing sulfuric acid can also be settled down as dry deposition. Thus, it is informative to study the combined composition of gases and particles for volcanogenic pollution and their impact on local area. However, to date, few studies on particulate matter, especially the size-segregated particulate matters, have been carried out in this volcanic region (Kinoshita, 2000; Kinoshita and Togoshi, 2000). Hence, relatively little is known about the composition of size-resolved particles and their relationship to gaseous materials. As a primary goal of this study, we report the chemical properties of the size-resolved particles collected nearby the volcanic crater of Sakurajima, Japan.
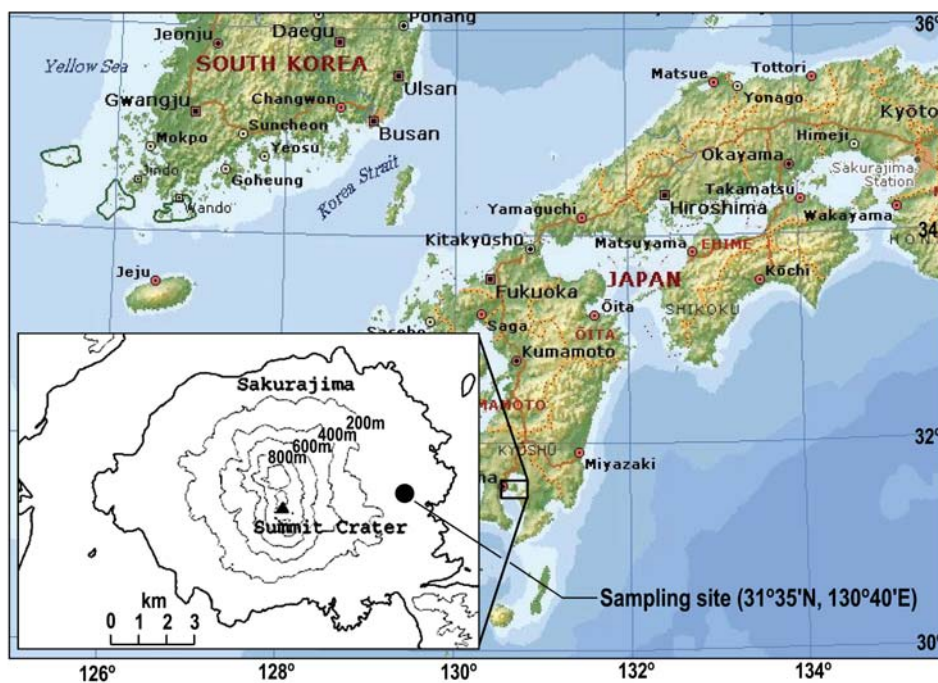
Fig. 1. Map showing the sampling site.

2. EXPERIMENTAL AND METHODS

2.1 Sampling of Size-resolved Particles

For the sampling of ambient particles, a three-stage multi nozzle cascade impactor (MCI®) (Tokyo Dylec Co.) was operated at a height of about 80 m above sea level of Kurokami observatory (31°35′N, 130°40′E) (Volcanic activity research center of Kyoto University) at the east part of Mt. Sakurajima in Kagoshima. This size-resolved particle collection system operated at a flow rate of 20 L min^{-1} for 24-h interval from 18-29 November, 2005.

As one of the multi-stage particle sampling instruments, this MCI combined with the 1st and 2nd stages having 12-orifice and back-up stage was employed to measure the size distribution and mass concentration levels of liquid and solid particulate matter. Particles were sampled directly on substrate material arranged behind the jet-nozzles of a cascade impactor. For the collection of particle samples, the airflow was maintained at approximately 20 L min^{-1}. Three-stage filters were used for the collection of 3 particle-size fractions: (1) the first stage: giant ($>PM_{10}$) (a 47 mm diameter, non hole Nuclepore® polycarbonate filter), (2) the second stage: coarse ($PM_{10-2.5}$) (a 47 mm diameter, non hole Nuclepore® polycarbonate filter), and (3) back-up stage: fine ($PM_{2.5}$) fraction (a 47 mm diameter, quartz fiber filter). During the sampling period, the tem-

perature was around 6.4-18.7°C (average 12.9°C) with relative humidity around 34-91% (average 63.1%). During sampling period the range of wind speed was 0.1-7.8 m s^{-1} and it was generally blowing from the west and southwest.

2.2 Analytical Equipments and Methodology

After sampling, all filters were placed in clean polyethylene petridishes and wrapped up with aluminum foil for refrigeration until analysis. Blank filters were handled in the same manner as the samples. For the laboratory analysis, these filters were extracted with deionized water by ultrasonic treatment. Ion Chromatography (IC) (Dionex DX-100) was used to determine the concentrations of various ions present in the size-resolved particles. Samples were analyzed for both cations (sodium, ammonium, potassium, magnesium and calcium) and anions (fluoride, chloride, nitrate, phosphate and sulfate).

2.3 Data Validation

To assure the reliability of our measurement technique, the quality assurance and quality control (QA/QC) was conducted by analyzing a set of known standard species. The data obtained by IC analysis were tested for precision by checking the relative standard deviation (% RSD) of each concentration of standard solution. In probability theory and statistics, the % RSD
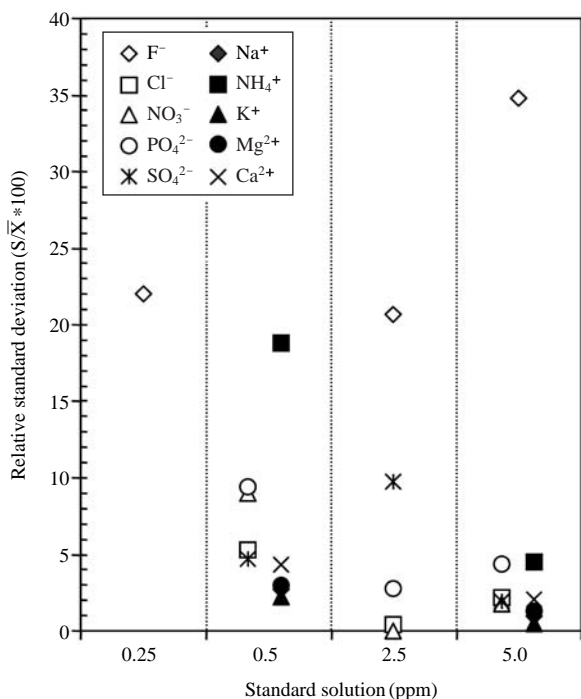
Fig. 2. Relative standard deviation of ionic species in each step of standard solution.

Fig. 3. Regression scatter plots of sum of anions versus sum of cations in $PM_{2.5}$.

refers to the absolute value of the coefficient of variation expressed as a percentage. In Fig. 2, most ionic components generally maintained low % RSD level. This result indicates that the absolute values of standard solutions did not vary significantly from each other. However, relatively high % RSD values were seen in the cases of fluoride (from 20 to 35%) and 0.5 ppm ammonium (18.5%) standards. The regression plot used for anion and cation balance, shown in Fig. 3, clearly shows that these ionic measurements are highly correlated, with the regression coefficient of 0.98. Although the analytical processes of IC employed in this study cannot determine the concentration of several minor anions (e.g. carbonate, bicarbonate, and water soluble organics like acetate, formate, etc.) the sums of equivalent concentration of anions for several samples are a little bit higher than those of cations. It is therefore suggested that these minor anions including their precursors were not significantly released from volcanic systems, and then they did not act on ion balance.

3. RESULTS AND DISCUSSION

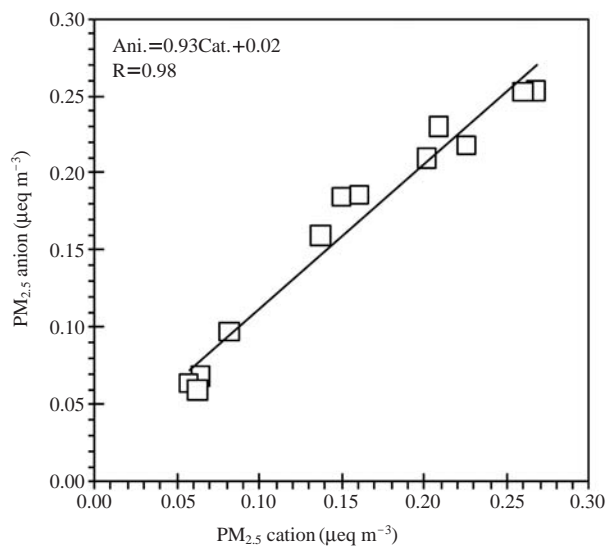To examine the transport and dispersion of the volcanic aerosol particles in the atmosphere, we ran the time dependent 3-dimensional Volcanic Ash Forecast Transport And Dispersion (VAFTAD) model developed by the National Oceanic Atmospheric Administration (NOAA) Air Resources Laboratory (ARL) developed. The VAFTAD calculates transport and dispersion of volcanic aerosol particles from an ash column extending from the volcano summit to the column top. This model uses spherical particles of density 2.5×10^6 g m^{-3} with diameter ranging from 0.3 to 30 µm (Heffter and Stunder, 1993). The input data for model calculation are eruption time, coordinates (start point), and height of source. The forecast meteorological fields for VAFTAL model are routinely generated from National Centers for Environmental Prediction (NCEP) daily runs of the Global Forecast System (GFS) model and the North American Mesoscale (NAM) model. The model computation of the visual ash cloud includes the magnitude of the volcanic eruption as determined by an algorithm based on the ash column top height and column depth. A detailed model description of the VAFTAD was given by Heffter and Stunder (1993).

In this study the VAFTAL model was run four episodical days (24 Nov., 26 Nov., 27 Nov., and 28 Nov.) when showed relatively high $PM_{2.5}$ during whole measurement period. Fig. 4 shows an example 8-panel chart of the forecast visual ash cloud beginning at 0900 local time on 24 Nov. 2005. As displayed in Fig. 4, the time dependent (6 h after eruption (top) and 12 h after eruption (bottom)) volcanic aerosol particles cloud dispersion is shown. The VAFTAD simulation result (FL SURFACE-550) indicates that the volcanic aerosol particles plume bounded for the east part of
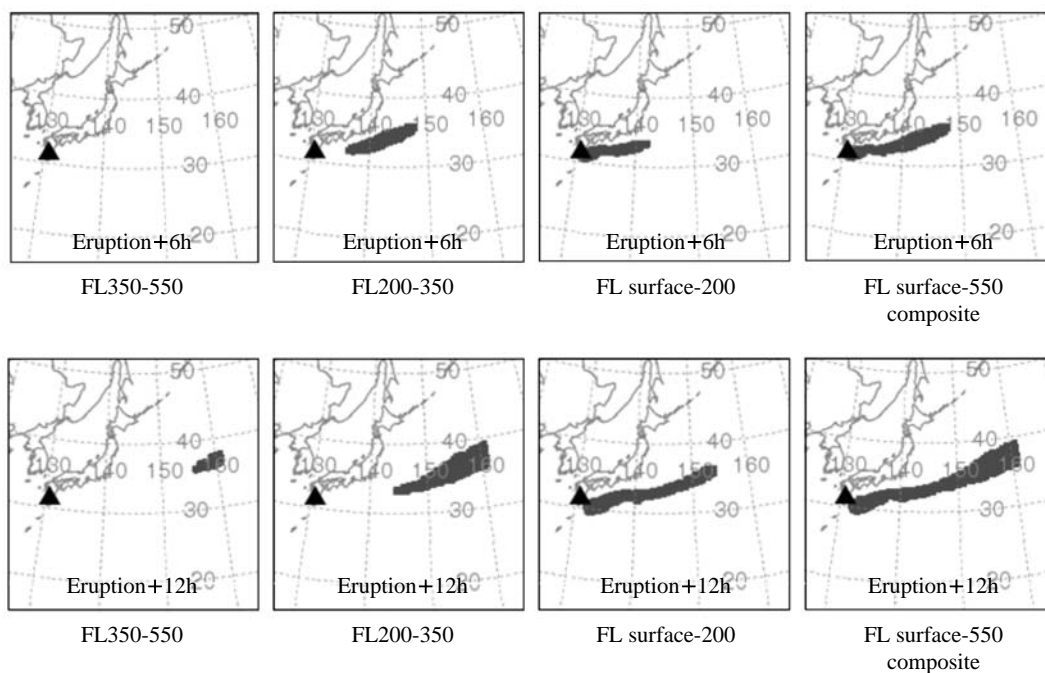
Fig. 4. VAFTAL model output of the forecast volcanic visual ash cloud erupted on Nov. 24, 2005. FL range means the upper and lower flight level. The right column panels are the composite layer, from the surface to FL550.
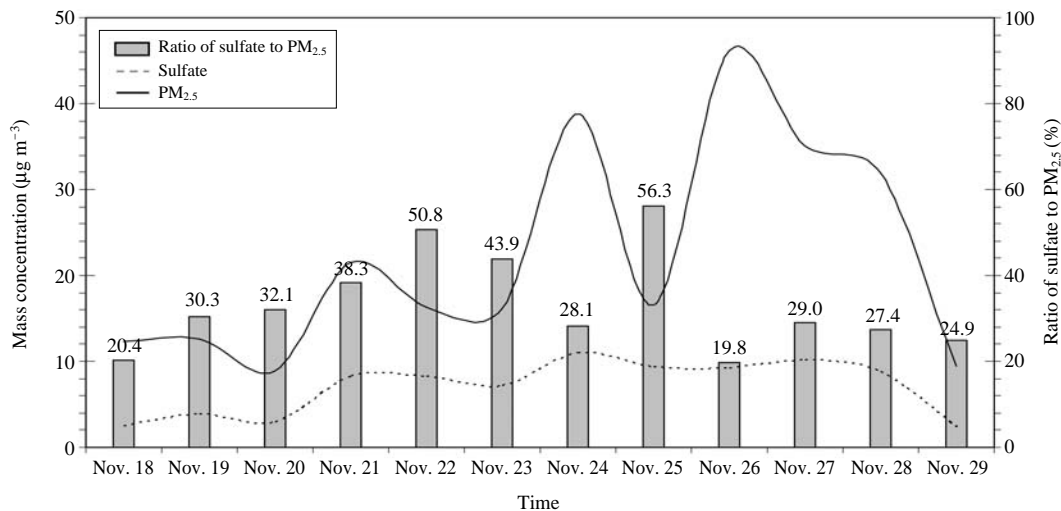

Fig. 5. Time series variation of the ratio of sulfate to $PM_{2.5}$ and concentrations of sulfate and $PM_{2.5}$ measured at Sakurajima.

Sakurajima for a while after eruption and then it moved toward to the Pacific Ocean. The visually described transport and dispersion of the volcanic aerosols also gives nearly the same results for other simulated model output. Thus, the present sampling site appeared to be affected by the volcanic aerosol particles plume.

Fig. 5 presents the temporal variations of sulfate and $PM_{2.5}$ and their ratio (sulfate to $PM_{2.5}$: indicated as bars) measured at Sakurajima during an intensive field measurement. The range of $PM_{2.5}$ concentration was between 8.9 and 46.1 $\mu g\ m^{-3}$ with an average of 22.1 $\mu g\ m^{-3}$. On the other hand, sulfate concentration varied from 2.3 to 10.9 $\mu g\ m^{-3}$ with an average of 6.94 $\mu g\ m^{-3}$. Both sulfate and $PM_{2.5}$ monitored during an intensive campaign showed a strong temporal varia- tion. The time resolution of $PM_{2.5}$ data collection allow-
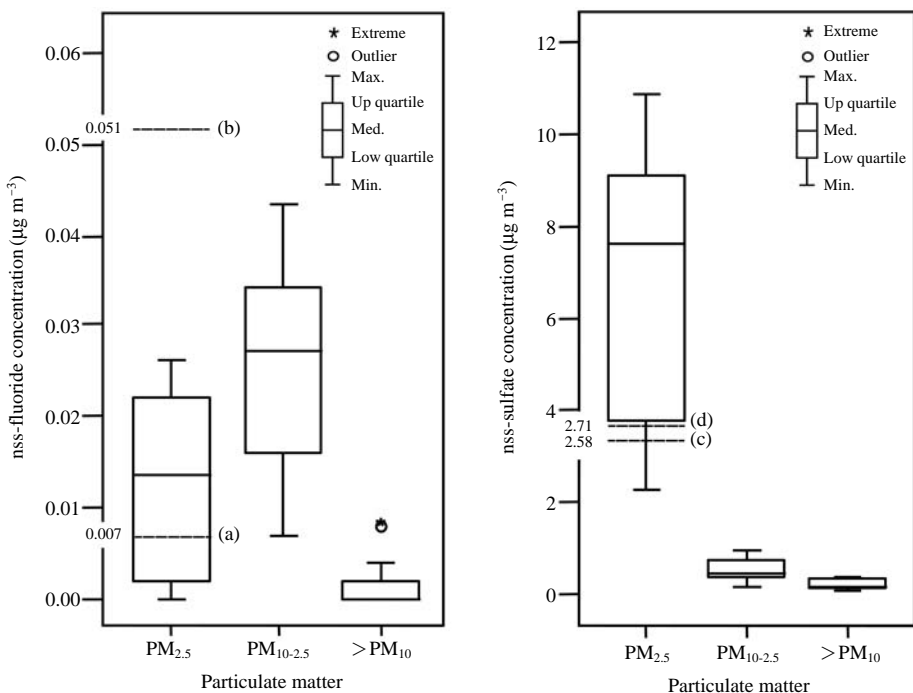
Fig. 6. Concentrations of nss-fluoride and nss-sulfate in size-resolved particulate matter colleced at Sakurajima.

ed us to identify episodes and to determine the eruption trends. The time series fluctuation of sulfate was moderately comparable to that of $PM_{2.5}$. The ratios of sulfate to $PM_{2.5}$ ranged between 19.8% and 56.3% with an average of 33.43%. Therefore, $PM_{2.5}$ mass concentration appears to be affected by the formation of sulfate thorough an eruption of the Sakurajima volcano. The ratio of sulfate to $PM_{2.5}$ found in this study is comparable to those of other background and urban areas. Moon *et al.* (2005) measured the chemical species in fine particulate matter at Gosan, Korea, one of the most representative background sites in the East Asia. The authors reported that the concentrations of $PM_{2.5}$ and sulfate were 21.3 and 3.39 $\mu g\ m^{-3}$, respectively to yield the $SO_4/PM_{2.5}$ ratio of 15.9%. Likewise the fine particles collected recently at an urban site in Korea showed average value of 38.9 $\mu g\ m^{-3}$ ($PM_{2.5}$) and 7.63 $\mu g\ m^{-3}$ (sulfate) and their ratio of 19.6%. (Park and Lim, 2006). The ratio of sulfate to $PM_{2.5}$ obtained in the volcanic site is thus higher than those of remote and urban sites.

Most fine sulfates occur due to the oxidation of sulfur dioxide gas. In humid atmospheres, oxidation typically occurs in clouds where sulfuric acid is formed within water droplets. If there is inadequate ammonia in the atmosphere to fully neutralize the sulfuric acid, then the resulting aerosols become acidic.

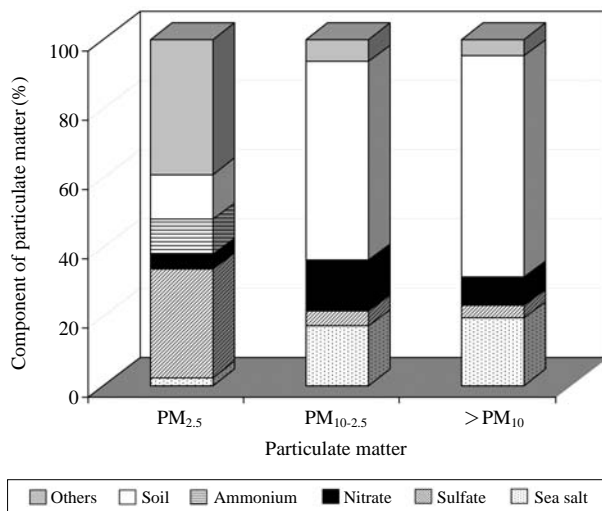As mentioned earlier, although a small amount of

Fig. 7. Percentage of mass loading in each size range.

hydrogen fluoride is released into the atmosphere from volcano, quantification of fluoride concentration in particulate matter should be meaningful to thoroughly examine volcanic activity. An intake of excess fluorine can act as a significant cause of death and injury in livestock during ash eruptions (Sutton and Elias, 1993). It also promotes acid rain effects downwind of volcanoes like HCl (Symonds *et al.*, 1994). As the ocean
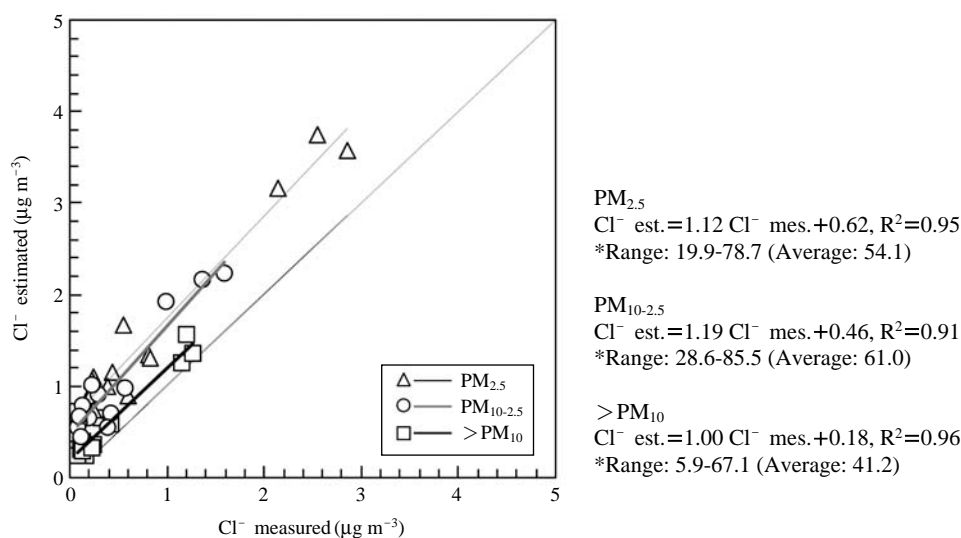
PM$_{2.5}$
Cl$^-$ est.=1.12 Cl$^-$ mes.+0.62, R^2=0.95
*Range: 19.9-78.7 (Average: 54.1)

PM$_{10\text{-}2.5}$
Cl$^-$ est.=1.19 Cl$^-$ mes.+0.46, R^2=0.91
*Range: 28.6-85.5 (Average: 61.0)

>PM$_{10}$
Cl$^-$ est.=1.00 Cl$^-$ mes.+0.18, R^2=0.96
*Range: 5.9-67.1 (Average: 41.2)

Fig. 8. Plotting of the measured vs. theoretical chlorides to estimate the chlorine loss. *[Cl$^-$]$_{loss}$(%)=([Cl$^-$]$_{est.}$−[Cl$^-$]$_{mea.}$)/[Cl$^-$]$_{est.}$ ×100.

water generally contains a very small amount of sulfur (0.27 wt%) and fluoride (1.3×10^{-4} wt%), non-sea-salt (nss) components were estimated in here. Fig. 6 shows the concentrations of nss-fluoride and nss-sulfate as a function of particle size. Their concentrations were also compared with the reference sites. As shown in Fig. 6, the concentrations of nss-F$^-$ and nss-SO$_4^{2-}$ exhibit not only strong particle size dependence but also dissimilar variation among three-step particle size to each other. The content of nss-F$^-$ was dominantly in PM$_{10\text{-}2.5}$, while that of nss-SO$_4^{2-}$ in PM$_{2.5}$. Although nss-F$^-$ had negligible concentration relative to nss-SO$_4^{2-}$, the occurrence of high nss-F$^-$ level in PM$_{10\text{-}2.5}$ may be ascribable to a pale yellow gas attached to fine ash particles during eruption. Fluorine also combines with metals to make fluorides (e.g., sodium fluoride and calcium fluoride). Nss-F$^-$ in PM$_{2.5}$ in the present study can be compared with those of rural and industrial areas in Ohio, U.S (Bates *et al.*, 1987). The median level of nss-F$^-$ in PM$_{2.5}$ collected at Athens, a rural area located approximately 105 km southeast of Columbus, Ohio, was 0.007 µg m^{-3}. On the other hand, that of Koebel located in the industrial center of the city consisting of foundries, plastic facilities, gravel/quarrying operations, and other manufacturing industries was 0.051 µg m^{-3} (http://www.epa.state.oh.us/dapc/atu/Section2 Chapter2.pdf). In fine fraction particles smaller than 2.5 µm, nss-F$^-$ concentration measured in the present work is relatively higher than that of rural site ((a) in Fig. 6). In contrast, in comparison to urban site ((b) in Fig. 6), it is very low. Human activities releasing fluorides into the environment are mainly the combustion of coal (containing fluoride

impurities) and other manufacturing processes (steel, copper, nickel, glass, brick, ceramic, glues and adhesives). Especially, aluminum smelters are sources of fluorides in various particle sizes (cryolite, aluminum fluoride, calcium fluoride, chiolite). In the case of nss-SO$_4^{2-}$ in PM$_{2.5}$, the level of present study (7.64 µg m^{-3}) is overwhelmingly higher than those of rural ((c) in Fig. 6) and industrial ((d) in Fig. 6) areas in Ohio, U.S.

The relative contributions of the five components to the size-segregated particles were examined. In Fig. 7, the percentages of their mass loading in each size range are exhibited. The amount of sea salts was derived from Na$^+$ concentration in aerosol and the Na$^+$ to total salt ratio of 0.306 in sea water (sea salt=3.27 × Na$^+$). Although in order to estimate the amount of soil fraction in aerosols, aluminum was generally selected as a tracer material of soil, the soil fraction in the present study was calculated by calcium concentration in ambient particles and the ratio of calcium to aluminum of reference (Gregory *et al.*, 1982). As explained already in the result of Fig. 5, the ratio of SO$_4^{2-}$ to PM$_{2.5}$ estimated in the present study is higher than those of rural and urban sites. This high ratio of SO$_4^{2-}$ to PM$_{2.5}$ might be caused by sulfate originated from the phase shift of SO$_2$ in volcanic gases. It is also possible to infer that a high contribution SO$_4^{2-}$ to PM$_{2.5}$ can reflect the positive artifact of quartz fiber filters which can effectively absorb SO$_2$. As might be expected, sea salt and soil fractions mainly contribute to the mass loading of coarse particles larger than 2.5 µm.

Among the acidic compounds detected in volcanic gases, SO$_2$ and NO$_x$ can participate in the chlorine loss to make the content of particle Cl$^-$ in the atmosphere
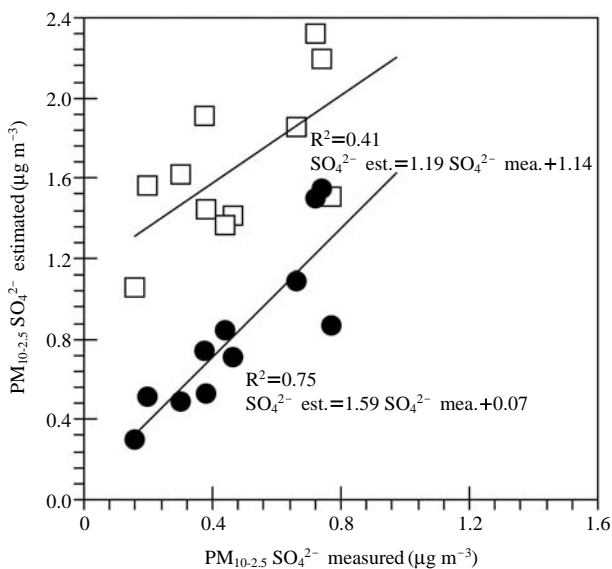
Fig. 9. Scatter plot of the measured SO_4^{2-} versus the theoretically calculated SO_4^{2-}-in PM_{10-25}. Empty squares are estimated SO_4^{2-} in $PM_{10-2.5}$ from Na_2SO_4, $MgSO_4$, and $CaSO_4$. Filled circles are estimated SO_4^{2-} in $PM_{10-2.5}$ from $MgSO_4$ and $CaSO_4$.

less than that of the sea salt. The chlorine loss may be caused either by the reaction of gaseous HNO_3 with NaCl in sea salt particles or by the reaction between H_2SO_4 and NaCl in sea salt. Fig. 8 illustrates the measured versus theoretically estimated chlorides in size-classified particulate matters. The estimated Cl^- mass concentration was theoretically calculated by $[Na^+$ mass concentration $\times 1.8]$. As shown in Fig. 8, all regression lines are far from the one-to-one line, suggests that the estimated Cl- concentrations are higher than the measured ones. This result indicates that chlorine loss occurred actively. The ranges of chlorine loss (%) in size-resolved particles were also calculated. It ranged from 20.0-78.8% with an average 54.1% in $PM_{2.5}$, whereas relatively high chlorine loss (28.6-85.5% with average 61%) was found in $PM_{10-2.5}$. The chlorine losses in $PM_{2.5}$ and $PM_{10-2.5}$ collected at Jeju Island, Korea were calculated as 32.4% and 39.6%, respectively (Moon *et al.*, 2005). As a consequence, the amount of chlorine loss calculated in the present study was relatively higher than that of remote site without volcanic activity.

Coarse particle fraction of sulfate in the atmosphere mainly exists in the form of Na_2SO_4, $MgSO_4$, and $CaSO_4$. Na_2SO_4 in coarse particles may be formed by the absorption of gaseous SO_2 in sea salt droplets due to its oxidation to H_2SO_4 and release of gaseous HCl from the sea salt;

$$2NaCl + H_2SO_4 \rightarrow Na_2SO_4 + 2HCl \uparrow$$
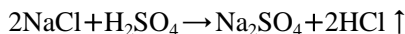
A thorough investigation of sulfate in coarse particles will be critical to understanding not only the existing types of sulfate but also the chlorine loss by sulfuric acid. Hence, the theoretically predicted concentrations of sulfate in $PM_{10-2.5}$, which showed the highest amount of chlorine loss in Fig. 8, were compared with the actually measured sulfate concentrations. Fig. 9 presents a scatter plot of $PM_{10-2.5}$ sulfate between the measured and theoretically calculated values. The latter was calculated by [concentration of counter ion $\times$ MW of sulfate/MW of counter ion]. Here, the counter ions are Na^+, Mg^{2+}, and Ca^{2+}. MW denotes molecular weight (in case of Na^+, MW was multiplied by two). As shown in Fig. 9, the theoretically calculated sulfate concentrations from Na_2SO_4, $MgSO_4$, and $CaSO_4$ were significantly overestimated. Moreover, their determination coefficient (0.41) was too low. On the contrary, the theoretically estimated sulfate concentrations from $MgSO_4$ and $CaSO_4$ had a relatively close relevance to the measured sulfate concentrations with a relatively good R square level (0.75). It can, therefore, reasonably be said that most sulfate in $PM_{10-2.5}$ are explained by $MgSO_4$ and $CaSO_4$. In other words, the Na_2SO_4 formed by the reaction between H_2SO_4 and NaCl in sea salt can be disregarded. If it is the case, the chlorine loss in $PM_{10-2.5}$ may be caused mainly by HNO_3 instead by H_2SO_4.

4. CONCLUSIONS

In this study, an intensive field measurement was conducted to elucidate the characteristics of size-classified ambient particles near the Sakurajima volcano in Japan. The time resolution data of sulfate and $PM_{2.5}$ concentrations with strong time serial variations allowed us to identify episodes and to determine the eruption trends during the intensive campaign. Sulfate concentration, which accounted for 31% of $PM_{2.5}$, seems to reflect oxidation of volcanically derived sulfur dioxide gas to sulfate particles. A comparison of the measured and theoretically estimated chlorides in size-segregated particulate matters suggested that the acidic compounds detected in volcanic gases can be actively engaged in chlorine loss. This chlorine loss, especially in $PM_{10-2.5}$ fraction, is suspected to be caused by HNO_3. Although a limited data were discussed, the data from our intensive field measurement helped us improve understanding of several important phenomena regarding the size-resolved particulate matters in volcanic region. However, to cope with the disaster of a volcanic eruption, it will be necessary to continue the monitoring of not only particulate matters but also gaseous mate-

rials.

REFERENCES

Bates, T.S., Cline, J.D., Gammon, R.H., Kelly-Hansen, S.R. (1987) Regional and seasonal variations in the flux of oceanic dimethyl sulfide to the atmosphere. Journal of Geophysical Research 92, 2930-2938.

Gregory, S.K., Glen, E.G., Scott, W.R. (1982) Identification of atmospheric particulate sources in Washington, DC using chemical element balances. Environmental Science Technology 16(2), 79-90.

Heffter, J.L., Stunder, B.J.B. (1993) Volcanic ash forecast transport and dispersion (VAFTAD) model. Weather Forecasting 8, 534-541.

Iino, N., Terada, A. (2003) Analysis of high volcanic gas concentrations at the foot of Miyakejima volcano, Japan. Journal of National Disaster Science 25, 85-91.

Kinoshita, K. (2000) Volcanic smoke/gases and atmospheric environment. Applied Meteorological and Climate Resources 13, 61-65. (in Japanese)

Kinoshita, K., Togoshi, H. (2000) Rise and flow of volcanic clouds observed from the ground and from satellites. Journal of Visualization 3, 71.

Luria, M., Peleg, M., Sharf, G., Tov-Alper, D.S., Spitz, N., BenAmi, Y., Gawii, Z., Lifschits, B., Yitzchake, A., Seter, I. (1996) Atmospheric sulfur over east Mediterranean region. Journal of Geophysical Research 101, 25917-25930.

Moon, K.J., Han, J.S., Kong, J.B., Lee, M.D., Jung, I.R. (2005) Characteristics of chemical species in gaseous and aerosol phase measured at Gosan, Korea during ABS-EAREX2005. Journal of Korean Society for Atmospheric Environment 21(6), 675-687. (in Korean)

Ohio Environmental Protection Agency (2003) Characterization of $PM_{2.5}$ in central and southeast Ohio, http:// www. epa. state.oh.us/dapc/atu/Section2Chapter2.pdf.

Park, J.Y., Lim, H.J. (2006) Characteristics of water soluble ions in fine particle during the winter and spring in Daegu. Journal of Korean Society for Atmospheric Environment 22(5), 627-641. (in Korean)

Sutton, A.J., Elias, T. (1993) Volcanic gases create air pollution on the Island of Hawaii: U.S., Geological Survey Earthquakes and Volcanoes 24(4), 178-196.

Symonds, R.B., Rose, W.I., Bluth, G., Gerlach, T.M. (1994) Volcanic gas studies: methods, results, and applications, Mineralogical Society of America Reviews in Mineralogy 30, 1-66.